Supplementary Figures

A

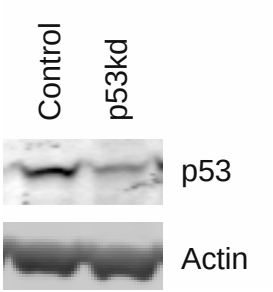

B

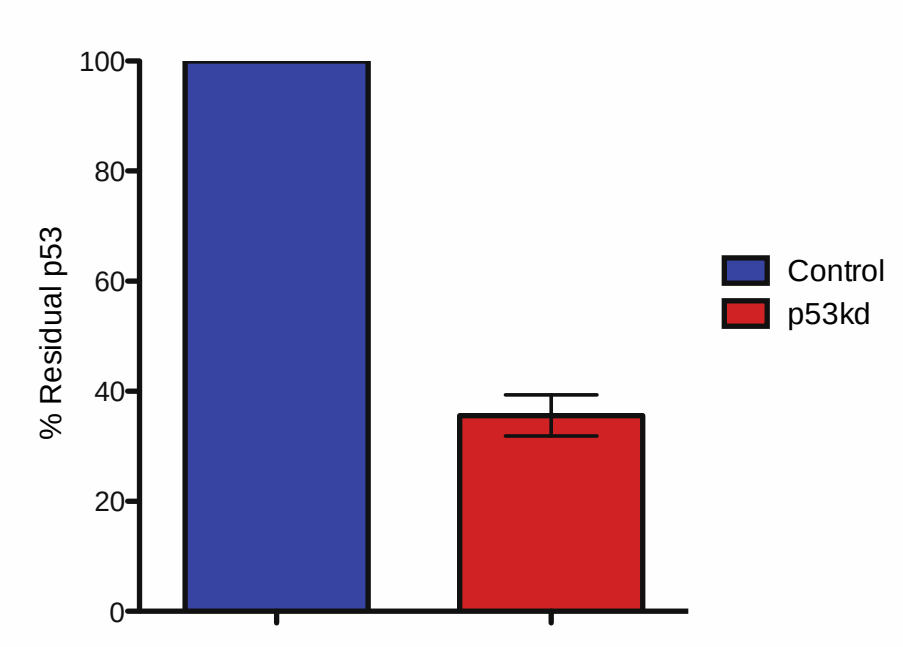

Supplementary Figure S1. p53 levels in p53 knockdown GBM cells.

(A) Immunoblot of p53 levels in Control and p53kd cells

(B) Quantification of p53 levels in Control and p53 knockdown cells (Error bars denote standard error of the mean, n=3).

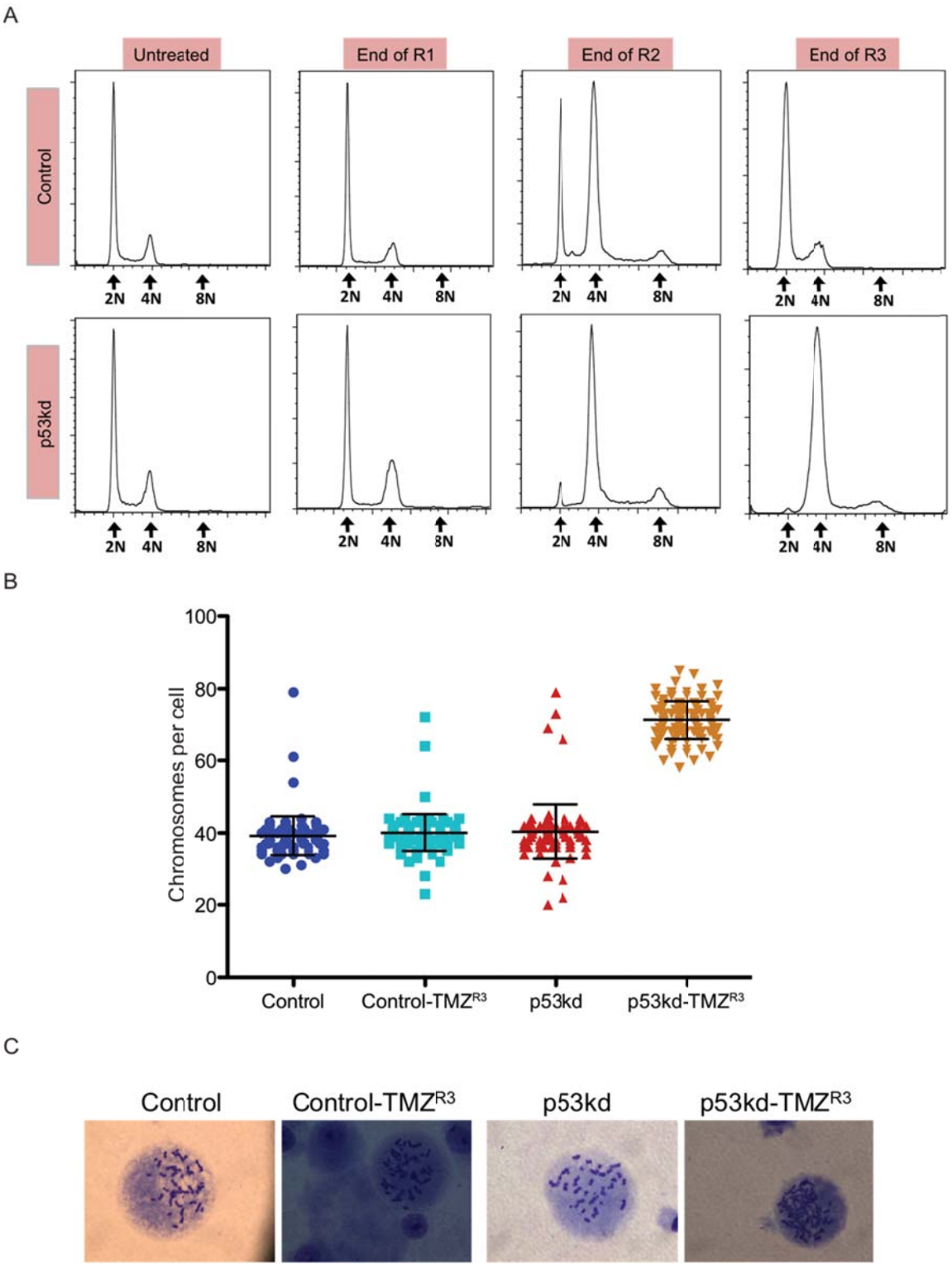

Supplementary Figure S2. TMZ^{R3} cells obtained from a p53 deficient background display increased ploidy.

(A) Cell cycle profiles of Control and p53kd prior to and after the first (R1), second (R2) and third (R3) rounds of TMZ selection.

(B) Quantitation of modal chromosome number from karyotypes of parental and TMZ^{R3} GBM cells (Error bars denote standard deviation from the mean).

(C) Representative karyotypes from p53kd and p53kd-TMZ^{R3} GBM cells.

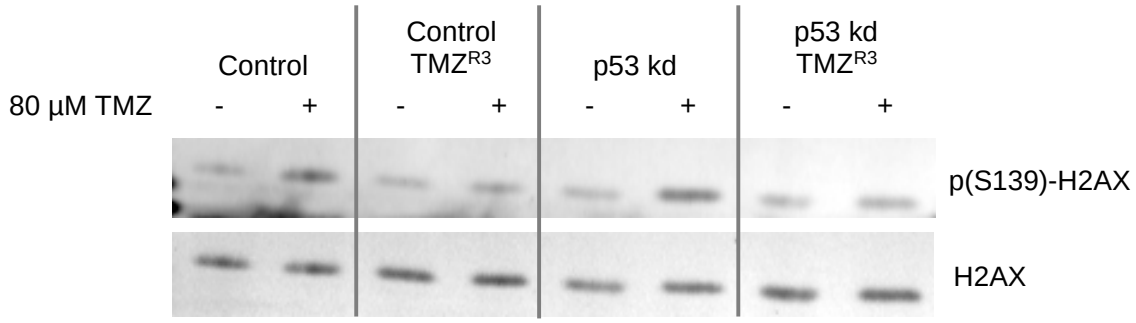

Supplementary Figure S3. H2AX activation in temozolomide treated parental and TMZ^{R3} GBM cells.

Immunoblot of serine 139 phosphorylated and total H2AX levels two cell cycle times after mock or 80 µM TMZ treatment

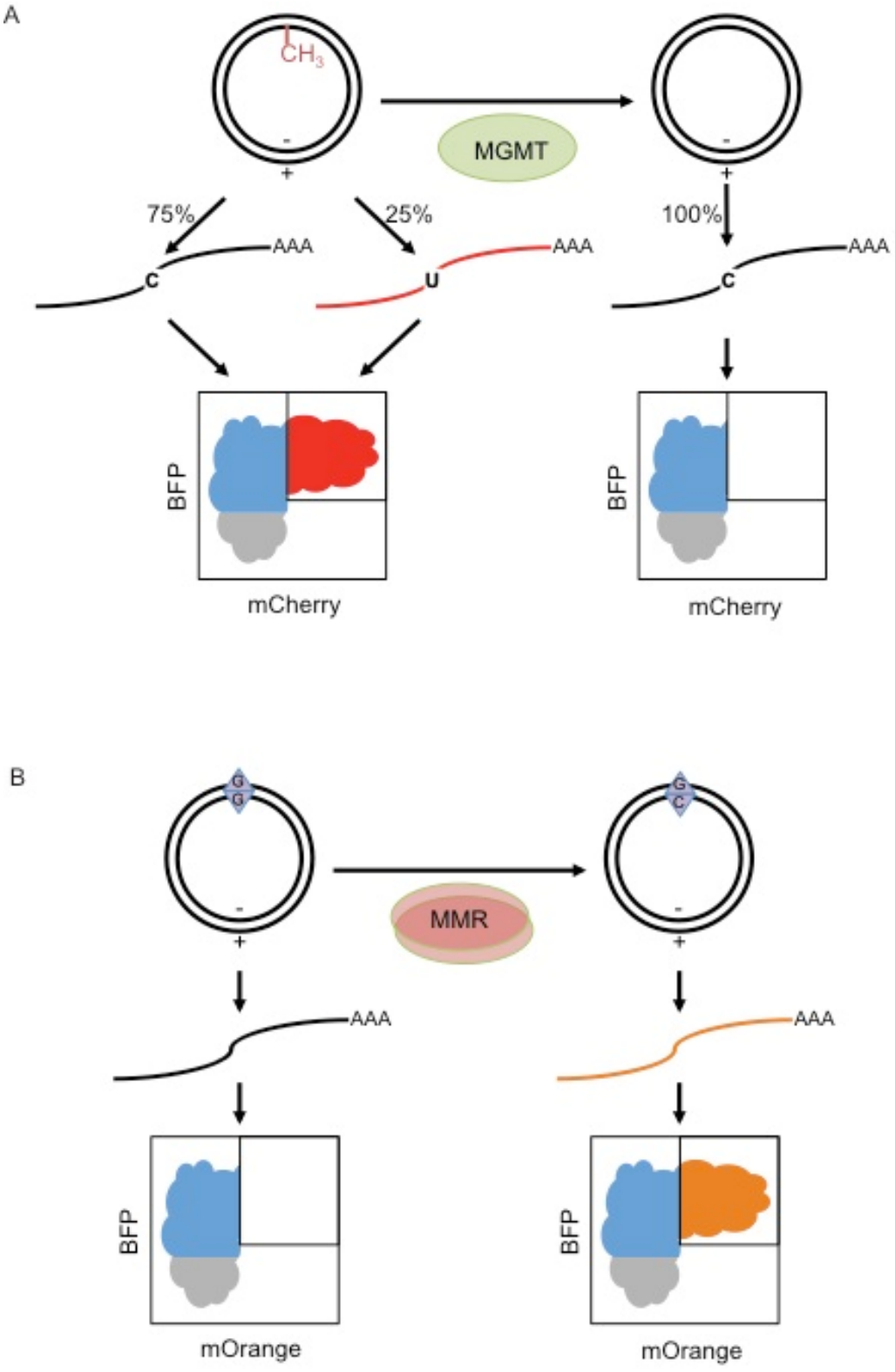

Supplementary Figure S4. In-cell Host cell reactivation (HCR) assays used to assess the MGMT and MMR repair capacity of GBM cells.

(A) Direct Reversal of O^6-meG HCR (DR-HCR). This assay reports on the ability of cells to repair a single O^6-meG lesion in the transcribed strand of a plasmid encoding a red fluorescent protein. Further details can be found in the Supplementary Materials and Methods section.

(B) Mismatch repair HCR (MMR-HCR). This assay reports on the ability of cells to repair a single G-G mismatch found in the template strand of a plasmid encoding an orange fluorescent protein. Further details can be found in the Supplementary Materials and Methods section.

A

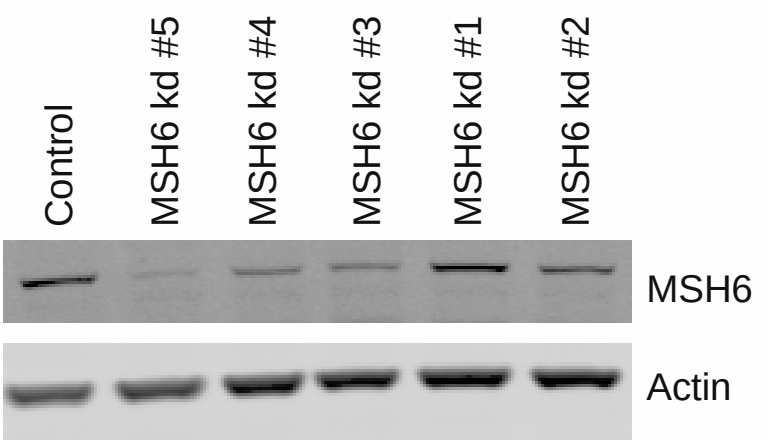

B

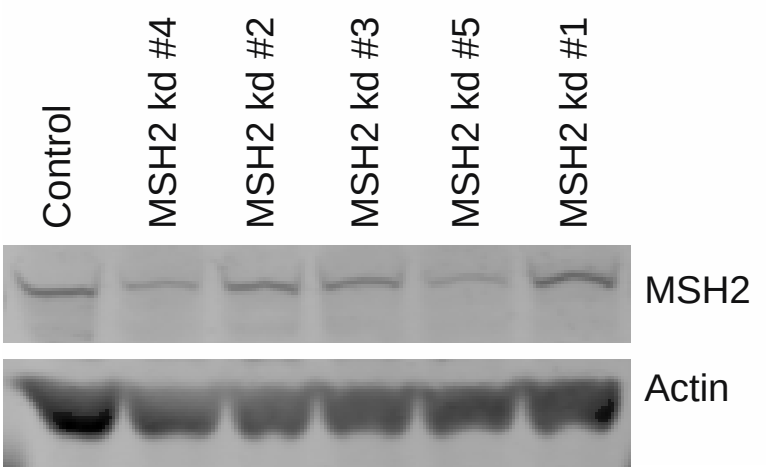

Supplementary Figure S5. MSH6 and MSH2 levels in MSH6 and MSH2 knockdown GBM cells.

(A) Immunoblot for MSH6 levels in MSH6 knockdown cells

(B) Immunoblot for MSH2 levels in MSH2 knockdown cells

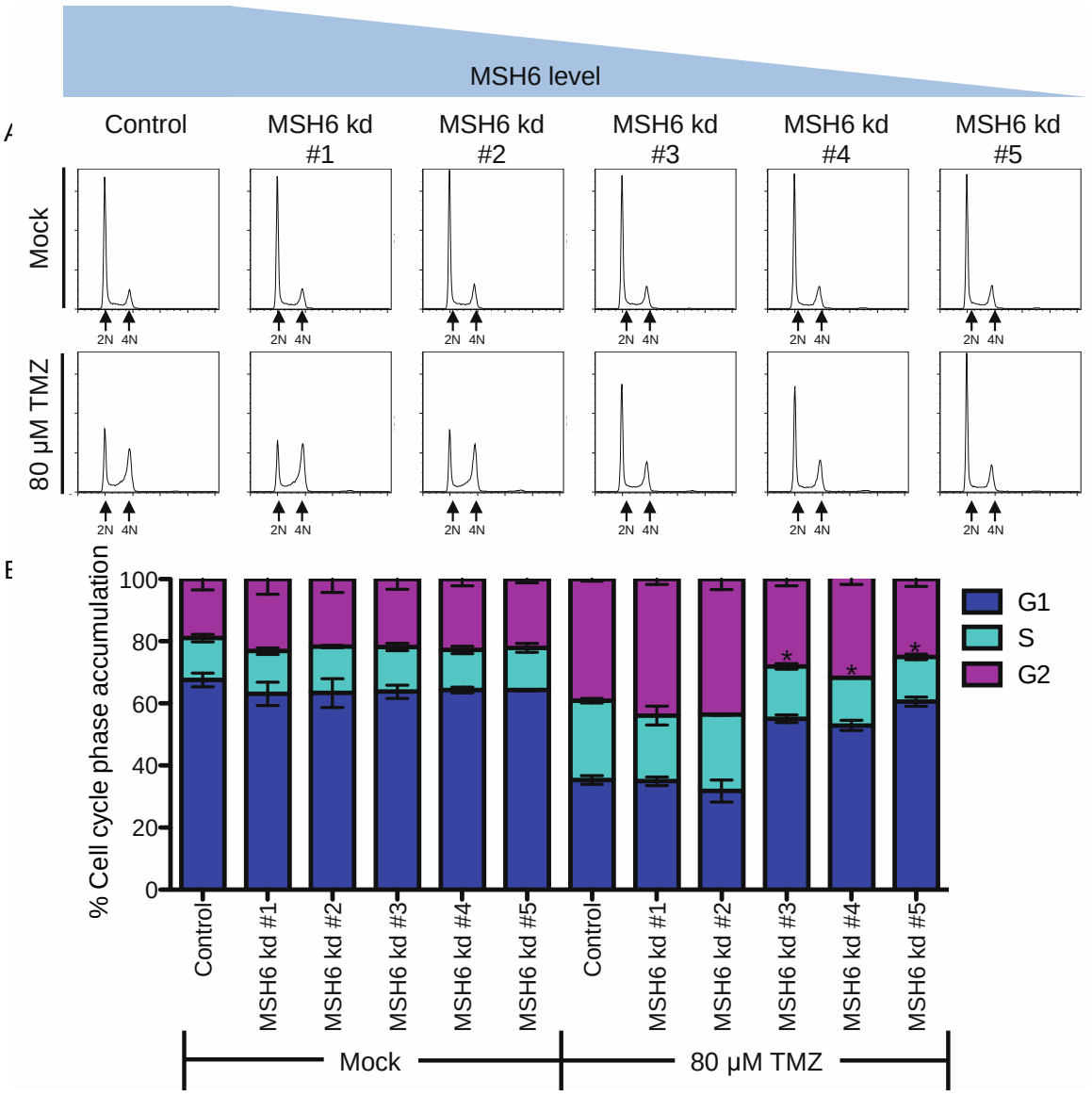

Supplementary Figure S6. Cell cycle profiles and quantitation of cell cycle changes in TMZ-treated MSH6 knockdown cells two cell cycle times post-TMZ treatment.

(A) Cell cycle profiles of mock or TMZ treated Control and MSH6 knockdown cells two cell cycle after treatment (B) Quantitation of the cell cycle changes in mock or TMZ treated Control and MSH6 knockdown cells two cell cycle after treatment (Error bars denote standard deviation from the mean of two independent experiments)

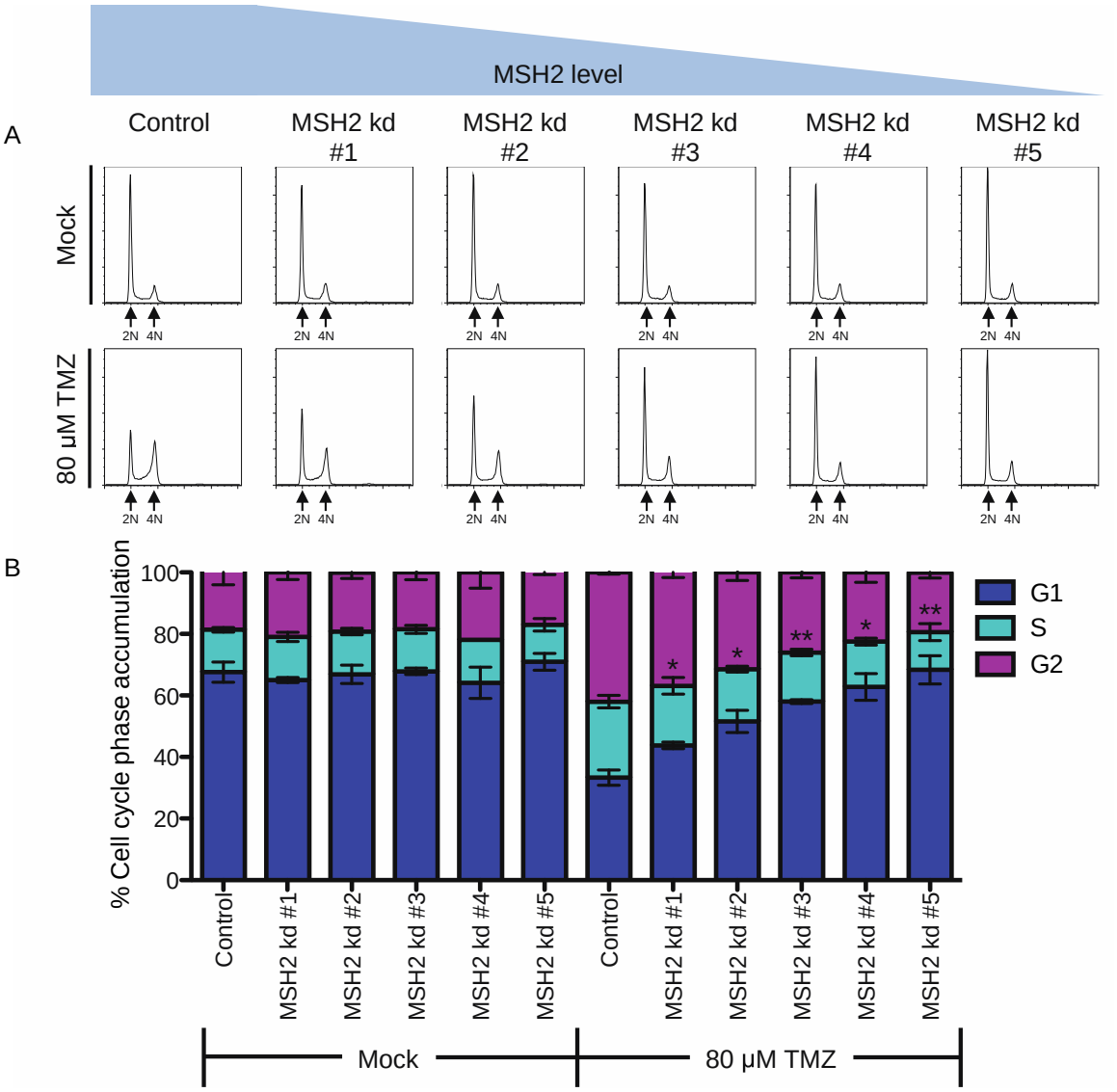

Supplementary Figure S7. Cell cycle profiles and quantitation of cell cycle changes in TMZ-treated MSH2 knockdown cells two cell cycle times post-TMZ treatment.

(A) Cell cycle profiles of mock or TMZ treated Control and MSH2 knockdown cells two cell cycle after treatment. (B) Quantitation of the cell cycle changes in mock or TMZ treated Control and MSH2 knockdown cells two cell cycle after treatment (Error bars denote standard deviation from the mean of two independent experiments).

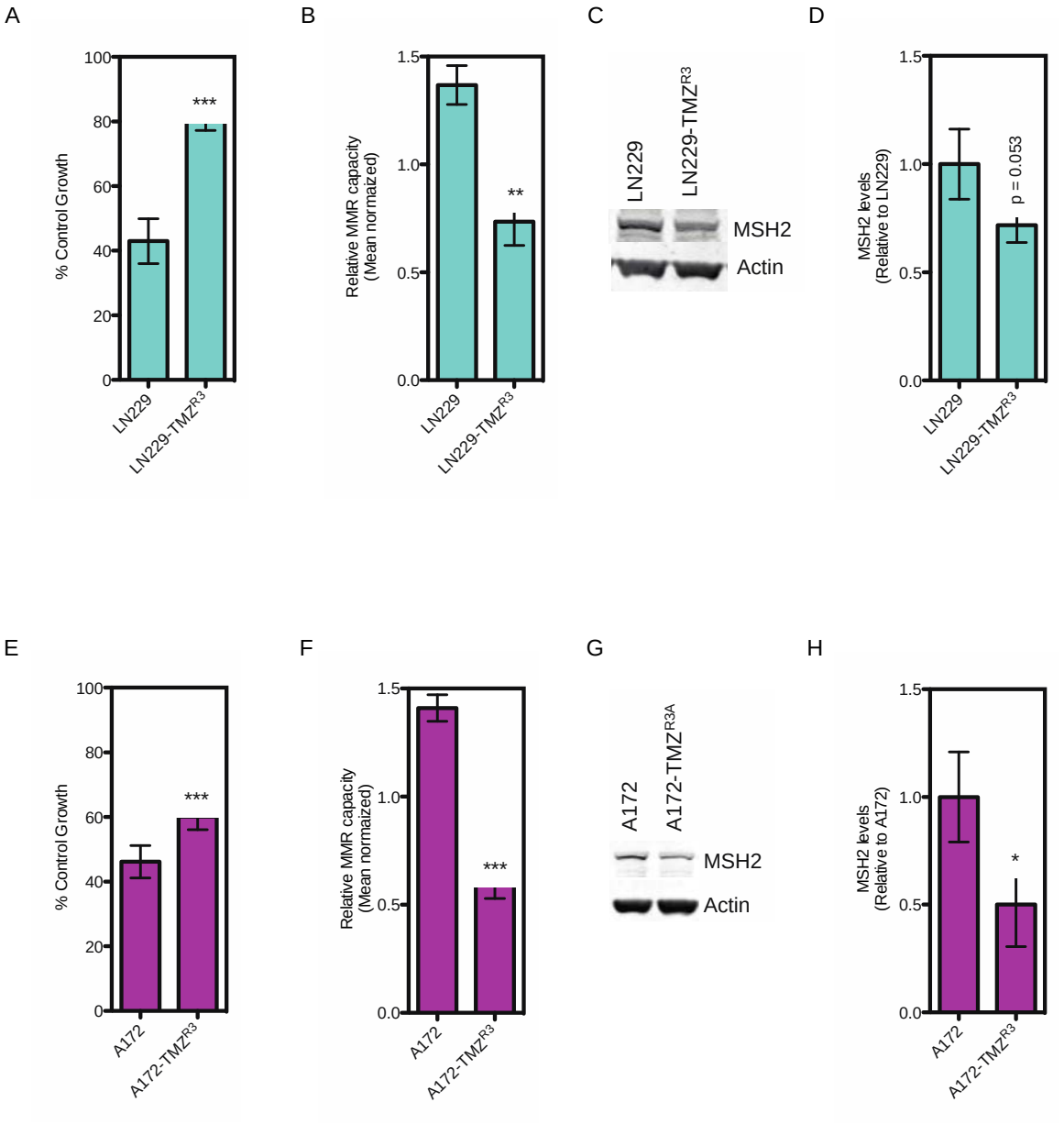

Supplementary Figure S8. Minor decreases in MSH2 levels correlate with acquired TMZ resistance in LN229 and A172 GBM cells.

(A/E) Sensitivity of parental and TMZ^{R3} LN229 (A) and A172 (E) cells to TMZ. Students t-test was used to assess significance between the sensitivity of parental and TMZ^{R3} GBM cells (Error bars denote standard deviation from the mean, n=5, *** p<0.001).

(B/D) Mismatch repair capacity against a G:G mismatch in parental and TMZ^{R3} LN229 (B) and A172 (F) cells (Error bars denote standard deviation from the mean, n=3,** p <0.01, *** p<0.001).

(C/G) Immunoblot of MSH2 levels in parental and TMZ^{R3} LN229 (C) and A172 (G) cells.

(D/H) Quantitation of MSH2 (C/G) immunoblots. Protein levels were normalized to MSH2 levels in parental LN229 (D) and A172 (H) cells (Error bars denote standard deviation from the mean, n=3, * p<0.05).

A

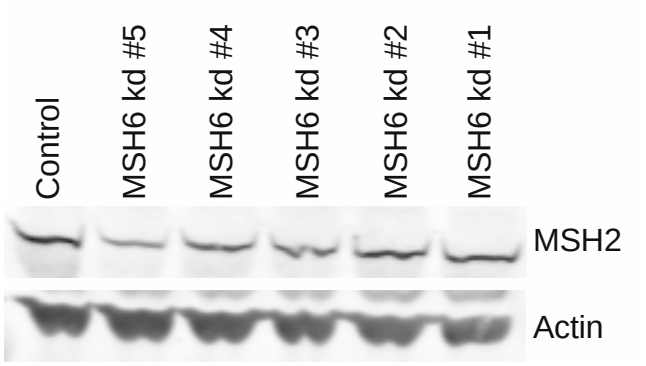

B

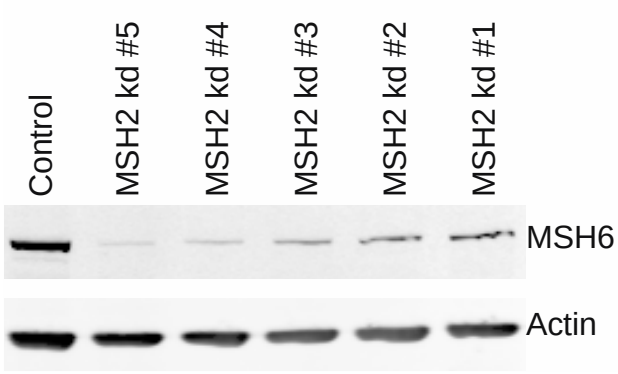

Supplementary Figure S9. Effects of MSH6 or MSH2 knockdown on the protein level of its dimerization partner.

(A) Immunoblot for MSH2 levels in MSH6 knockdown cells

(B) Immunoblot for MSH6 levels in MSH2 knockdown cells

A

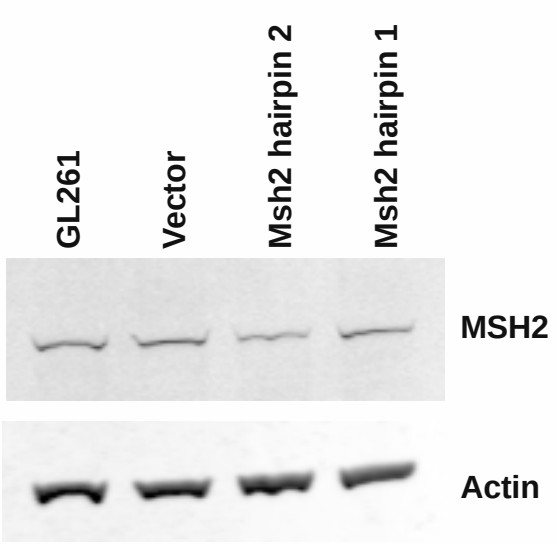

B

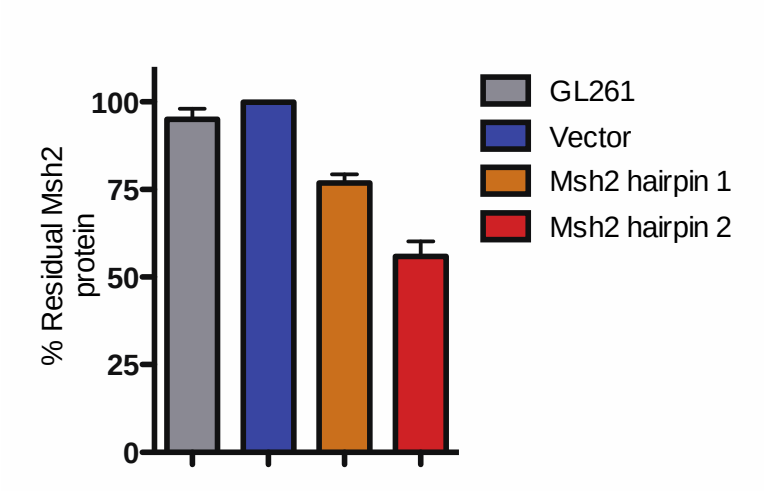

Supplementary Figure S10. *Msh2* knockdown in GL261 glioblastoma cells.

(A) Immunoblot for Msh2 protein levels in parental GL261 cells and cells expressing either a vector control of a short hairpin RNA targeting *Msh2* transcripts.

(B) Quantification of Msh2 protein levels in parental GL261 cells and cells expressing either a vector control of a short hairpin RNA targeting *Msh2* transcripts (Error bars denote standard deviation from 3 independent experiments).

A.

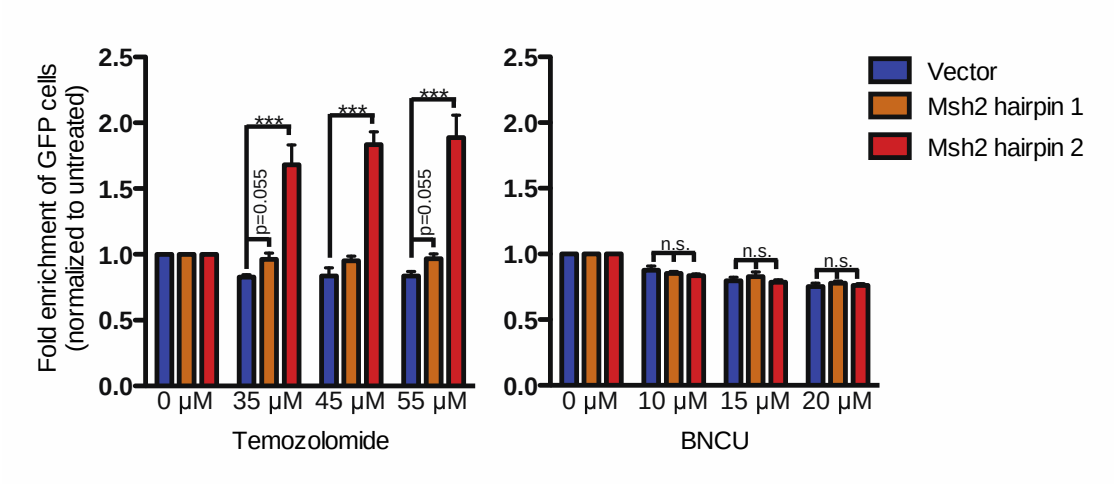

B.

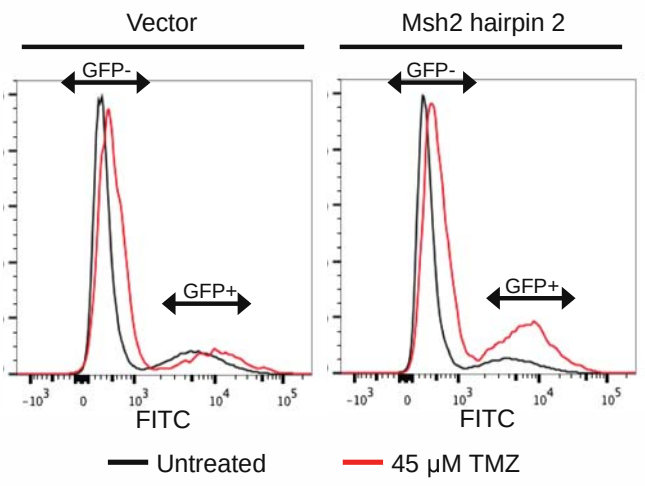

C.

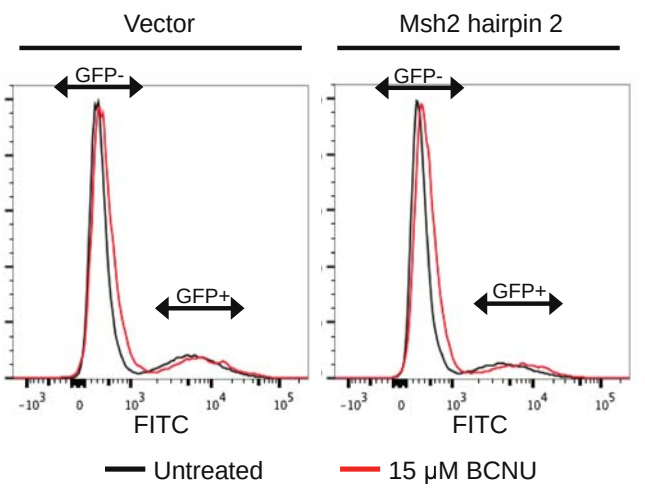

Supplementary Figure S11. Moderate decreases in *Msh2* confer a growth advantage to GL261 GBM cells after TMZ, but not BCNU, exposure *in vitro*.

(A) TMZ and BCNU induced changes in the proportion of GFP expressing cells in GL261 GBM cells expressing a vector control or one of two hairpins targeting *Msh2* transcript as measured *in vitro*. Flow cytometry was used to assess changes in the percentage of GFP positive cells 96 hours post-TMZ treatment (n=3, ± s.e.m., p< 0.05*; 0.001***; n.s. not significant Student's t-test).

(B/C) Representative histograms from TMZ (B) or BCNU (C) treated GL261 GBM cells expressing either Vector or Msh2 hairpin 2 and a marker GFP.

A

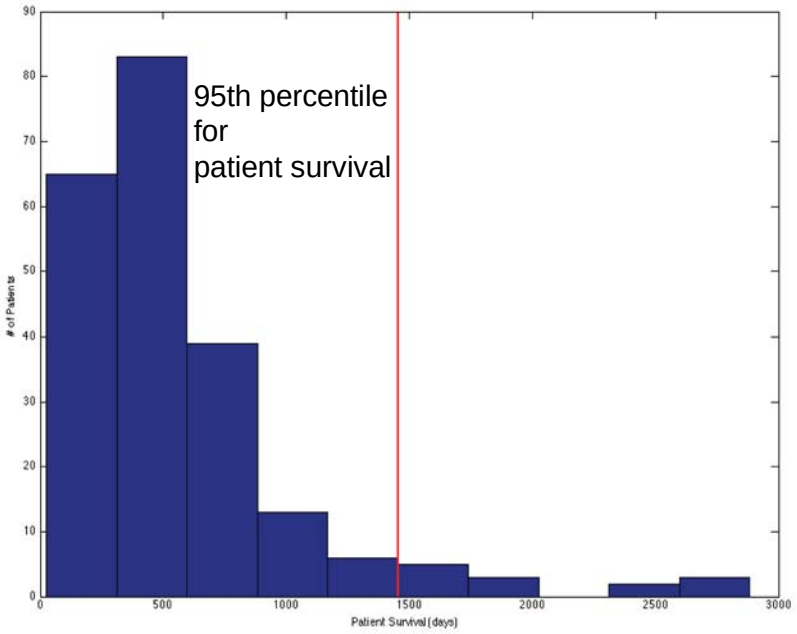

B

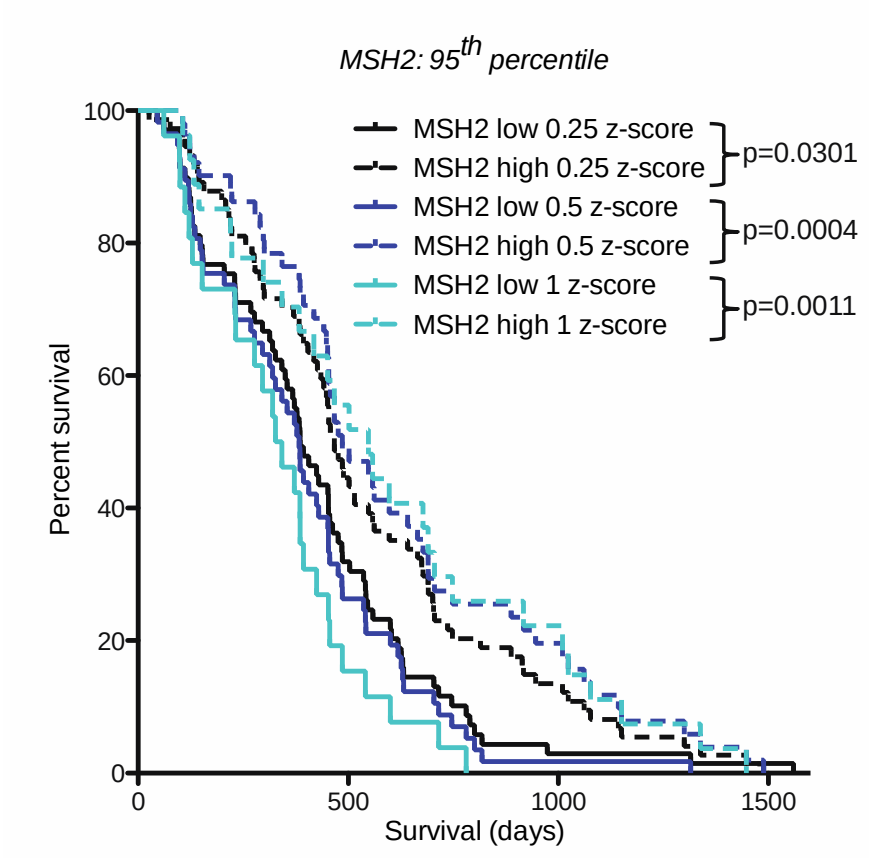

Supplementary Figure S12. Distribution of patient survival in TMZ treated TCGA GBM patients and effects of MSH2 transcript levels on the survival of TMZ treated

patients in the 95th percentile for patient survival after TMZ therapy.

(A) Histogram depicting the survival of TMZ treated GBM patients. Survival data was obtained from the clinical data set for GBM patients in the NIH TCGA data matrix. The vertical red line demarcates the separation of the patients who fall into the upper 5th percentile for patient survival after TMZ treatment.

(B) Overall survival of GBM patients defined as high or low MSH2 at various z-score cutoffs. The log rank test was employed to assess significance between the median survivals of both populations.

A

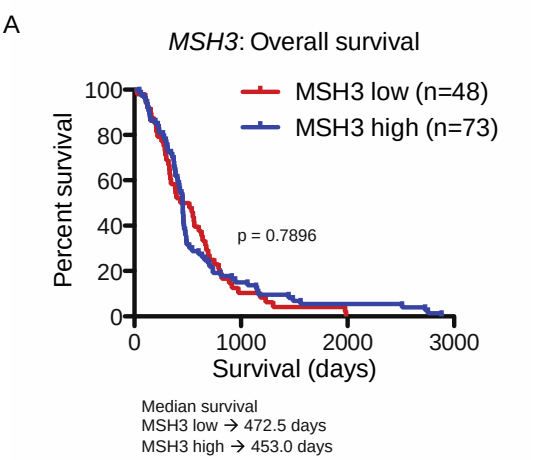

B

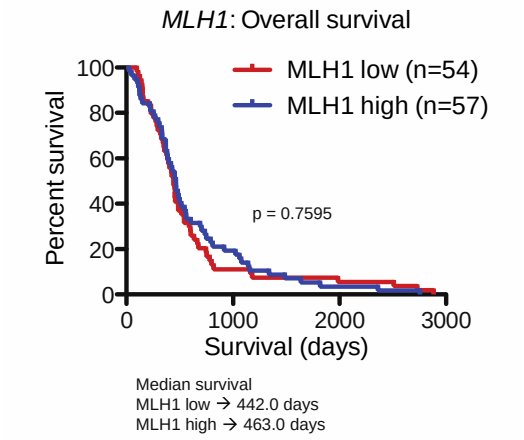

C

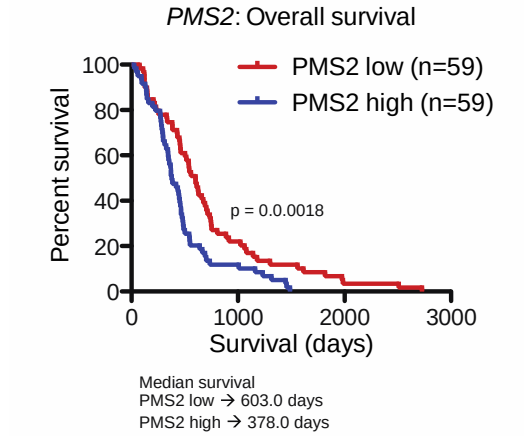

Supplementary Figure S13. Overall survival of GBM patients stratified by MSH3, MLH1 and PMS2 tumor transcript levels. (A-C) Overall survival of GBM patients stratified as high or low MSH3 (A), MLH1 (B) and PMS2 (C) expressers using a z-score

cutoff of 0.5. The log rank test was employed to assess significance between the median survivals of both populations.

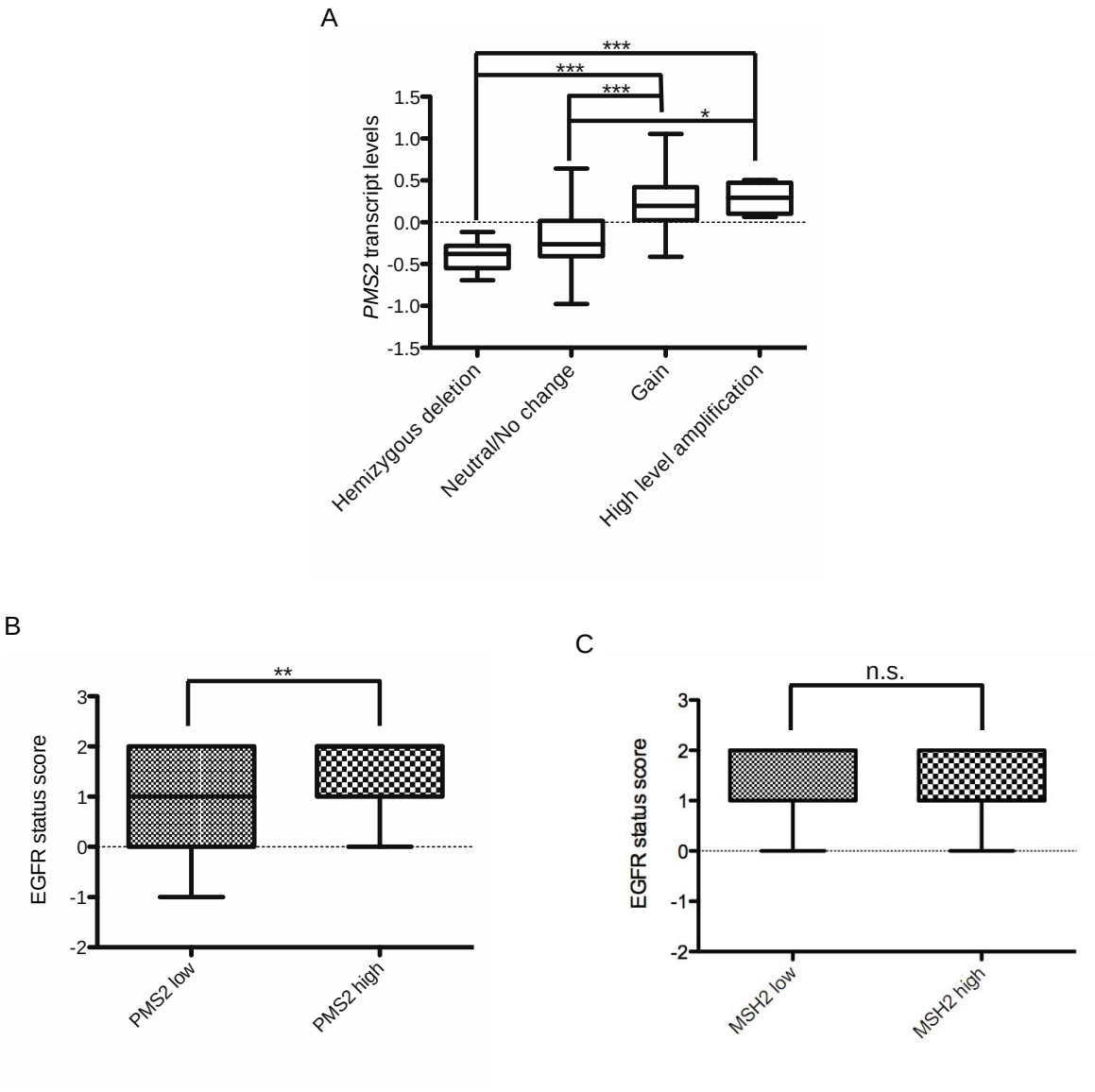

Supplementary Figure S14. *PMS2* transcript levels correlate with increased chromosome 7 copy number.

(A) *PMS2* transcript levels as a function of PMS2 copy number. Copy number data for TCGA patients was obtained from cBioportal.

(B-C) EGFR copy number in TMZ treated patients of varying *PMS2* (B) or *MSH2* (C) levels. EGFR status score was calculated based on the TCGA copy number scoring as follows; -1 hemyzygous deletion, 0 Neutral/No change, 1 Gain, 2 High-level amplification (whiskers on the box plots denote the minimum and maximum values).